# MEASUREMENT AND MODELING OF THE 5 GHZ AIRPORT SURFACE CHANNEL AT BARAJAS AIRPORT

*Tor Andre Myrvoll, Jan Erik Håkegård, SINTEF, Trondheim, Norway*

## Abstract

AeroMACS is a system currently under development to be used for airport surface communications. It is based on the IEEE802.16-2009 standard, and is developed in cooperation with the WiMAX forum. The frequency band allocated to AeroMACS is 5091-5150 MHz.

When specifying the AeroMACS system, knowledge of typical propagation conditions at airports is of importance. Typical path loss models are necessary to estimate the range of a transmitter within different zones of the airport, and typical fading characteristics are used to estimate the performance of e.g. the selected coding and modulation schemes.

## Introduction

In November 2010, channel measurements were conducted at the Barajas Airport in Madrid. The scope of these measurements was to develop new channel models, including both path loss and fading characteristics. There have been done channel measurements at airport environments previously, both in U.S. and in Europe. In [1,2], measurements involving several airports in the U.S. are reported and channel models based on the measurement data are derived. In [2], similar measurements from the Munich airport are reported. Common for both these measurement campaigns is that the base station was located at great height on top of control towers. This is a representative localization of the base station if the intention is to cover large parts of or the entire airport area. It is however expected that the capacity requirement at in particular large airports will be too large to be handled by one or a few base stations covering the entire airport surface. Moreover, much of the data traffic will be generated at gate areas of the airports. In this environment, the channel models developed in [1] and [2] will not be valid. The purpose of the Barajas campaign was to fill this gap, by doing measurements in the gate area.

Measurements were done for base station antennas at two different heights, and for a mobile station moving in non-line-of-sight (NLOS), in line-of-sight (LOS), and in a mix of LOS and NLOS environments. Path loss parameters as well as fading characteristics were then derived based on the measurements. The remaining sections of this paper are organized as follows. In the next section, the measurement campaign is briefly described. Then the results from the path loss modeling for NLOS and mixed NLOS and LOS conditions are given. In Section 4, fading characterization for the NLOS case is presented, before finally conclusions are drawn.

## Measurement Campaign

Measurements at the gate area were conducted with the base station attached to the West Tower of Barajas, which is one of the airport's three towers. The West Tower is located within the gates on the east side of Terminal 4 and is used for surface movements. Measurements were done first with the base station at the 2$^{nd}$ floor of the tower, and then at the 7$^{th}$ floor. These locations are in this publication called BS1 and BS2, respectively. BS1 is located 12 meters above ground, while BS2 is located 38 meters above ground.

The mobile terminal was installed in a vehicle, and measurements were done with the vehicle following three routes MR1, MR2 and MR3. MR1 went along the terminal building, and mainly provides NLOS conditions. MR2 went in between aircraft parked at the gates, and provides a mix of LOS conditions and NLOS conditions. Finally, MR3 encompassed taxiways, and provides primarily LOS conditions.

### *Antenna Characteristics*

The base station antenna was a 120 degree sector antenna with 15 dBi gain. The beamwidth in elevation was 6 degrees. The antenna was directed and tilted in order to keep as much as possible of the mobile routes within the main lobe of the antenna. However, the antenna for both BS1 and BS2 was located so far above ground that the antenna diagram

978-1-4577-0592-2/11/$26.00 ©2011 IEEE

needed to be compensated for for short distances between the base station and the mobile terminal. The antenna diagram from the data sheet of the antenna is provided in Figure 1. In order to compensate for the effects of the varying antenna gain, a first order sinc-approximation is used. The approximated antenna diagram is included in Figure 2.

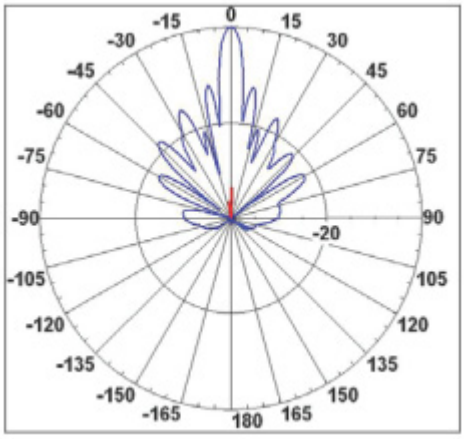


**Figure 1. BS antenna Diagram in Elevation**

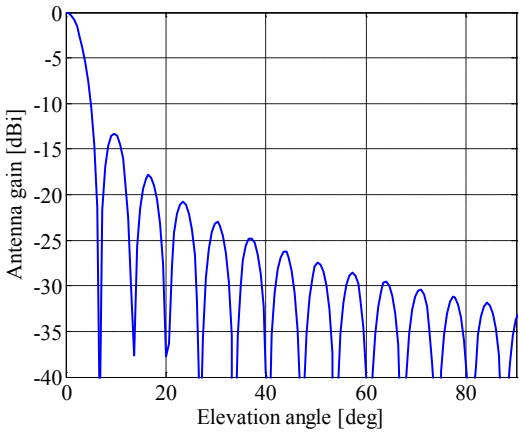


**Figure 2. Approximated BS Antenna Diagram**

On the mobile terminal side, a 6 dBi antenna that is omnidirectional in azimuth was used. No compensation of the path loss due to the mobile terminal antenna was considered as necessary.

## Path Loss Modeling

The path loss model follows the well known two slope model:

$$PL = \begin{cases} A + 20\log d\,, & d < d_{BP} \\ A + 20\log d_{BP} + 10\gamma \log\frac{d}{d_{BP}}, & d \geq d_{BP} \end{cases}$$

In the equation above, the constant is given by $A = 32.44 + 10\log f$ , where $f$ is the operating frequency in GHz ($d$ is in meters). The model then contains two parameters, the break point distance $d_{BP}$ and the path loss exponent $\gamma$. For shorter distances than the break point, free space path loss is assumed, while the slope of the path loss curve is determined by the path loss exponent for distances above the break point distance.

The path loss model is derived from measurements. Straight line linear regression is used to calculate the maximum likelihood estimator. Due to the effect of the antenna diagram, only distances above 200 meters are included in the calculations for BS1, and distances above 300 meters for BS2. The linear regression provides the path loss exponent $\gamma$. The break-point distance is then calculated by imposing that the path loss exponent below the breakpoint is equal to 2.

Figure 3 to Figure 6 contain measurement results for BS1 and BS2 and for the mobile routes MR1 and MR2. Also included is the calculated path loss model (blue stippled curves) and the path loss when the antenna gain is included (black curve).

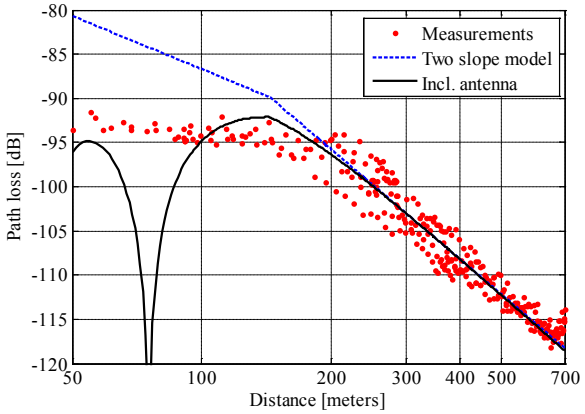


**Figure 3. BS1 MR1 Measurements and Model**

For BS1MR1 measurements, the mobile terminal was visible from the base station up to about 150 meters distance, when it disappeared below the nearest gate. Then it became visible for a short while before it disappeared below the more distant gates and remained invisible until the end of the terminal building about 700 meters away from the base station. Hence, for the major part of the route from about 150-200 meters to 700 meters, the route provided complete NLOS conditions. Figure 3 shows

that the measurements follow the path loss model with only small errors. The break point distance is 144 meters and the path loss exponent is 4.13.

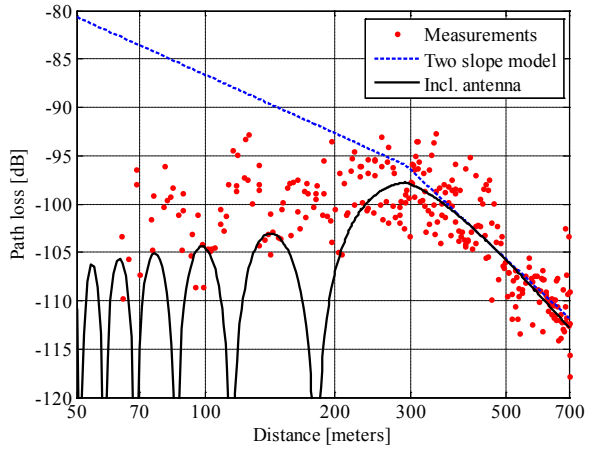


**Figure 4. BS2 MR1 Measurements and Model**

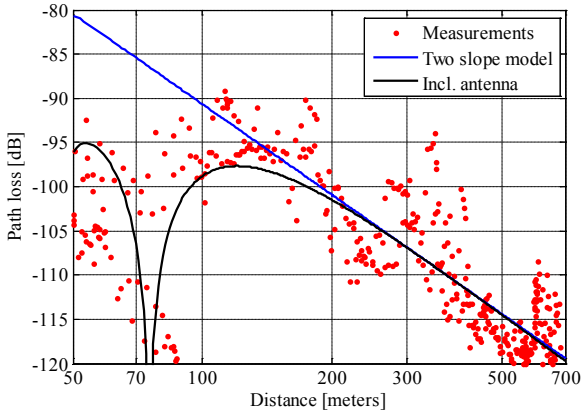


**Figure 5. BS1 MR2 Measurements and Model**

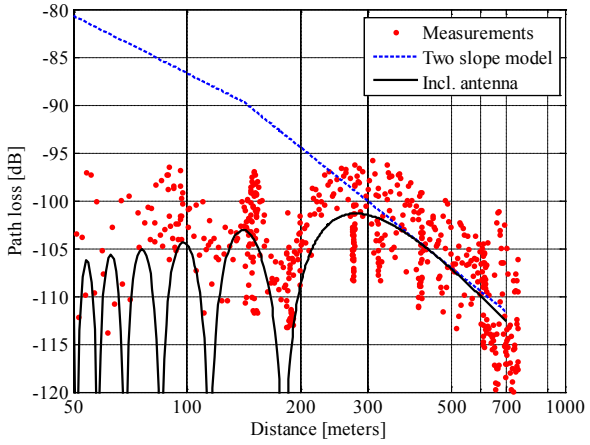


**Figure 6. BS2 MR2 Measurements and Model**

When the base station antenna is moved from 12 meters to 38 meters height (BS2), the mobile terminal remains visible between the gates for much longer distances. As the vehicle drives away from the base station, it becomes visible until it is about 5 or 6 gates away from the base station, corresponding to a distance of about 350 meters. For longer distances, it is mostly hidden underneath gates, although occasionally visible between gates, until it arrives at the end of the terminal building. The measurements are much more scattered in this case than for the BS1 measurements, as can be seen from Figure 4. The reason for this is mainly that the mobile terminal moves between LOS and NLOS conditions for a larger portion of the route, and also because more sharp reflections from the gates make the signal fluctuate. The path loss model has a larger break point distance (292 meters) than the BS1 measurements, but the path loss exponent for distances greater than the breakpoint is similar (4.15).

While the mobile route MR1 was well defined to follow a road along the terminal building, mobile route MR2 was more random, as it involved driving in the parking area of the aircraft. Hence, the exact route was affected by where there were aircrafts parked and where permission to drive was given. The mobile station remained out of sight from the base station antenna when the vehicle moved behind aircraft, and came into sight between aircraft. Hence, these measurements include a mix of LOS and NLOS measurements. Figure 5 shows how the measurements fluctuate. The path loss model provides the best straight line solution, but it is clear that the path loss at a given position will deviate greatly from the model. The partial LOS conditions of the channel do however lead to a lower path loss exponent (3.40) than for mobile route MR1. The break point distance is however shorter, so that the resulting path loss for the distances of most interest is quite close to those of MR1.

For MR2 measurements with the base station antenna at 38 meters height (BS2), the path loss measurements are quite different than those obtained with the lower antenna. The mobile terminal will be less hidden behind aircraft, and the average path loss is therefore smaller. This is reflected by both a larger break point distance (141 meters) and a smaller path loss exponent (3.15).

The results of the path loss modeling are summarized in Table 1 and illustrated in Figure 7. Several conclusions can be drawn from the curves.

- It is clear that increasing the height of the base station provides larger coverage. The range is increased by about 25 % by increasing the height from 12 meters to 38 meters.
- The path loss in all cases is significantly larger than the free space path loss. Even for BS2 located 38 meter above the surface, a distance of 500 meters leads to about the same path loss as a distance of 1000 meters in free space. BS1 located 12 meters above the surface provides the same path loss at about 300-350 meters.
- For short distances, MR1 provides less path loss than MR2, while the difference is small for larger distances. This is due to the actual surroundings of the base station locations. For small distances, there were good LOS conditions in the direction MR1 until a certain point, after which there where complete NLOS (BS1) or close to NLOS (BS2). In the direction of MR2 however, there were some obstructions relatively close to the base station, while there were partly LOS conditions until the end of the route.
- The mean square error (MSE) is small for BS1MR1, illustrating good match between the data and the path loss model. This is because the data is obtained in pure LOS conditions. For BS1MR2, and even more so for BS2MR1 and BS2MR2, the MSE is large, illustrating that there is not a good match between the data and the model. By correlating the path loss measurements and the delay spread measurements, a more complex model containing a LOS state and a NLOS state in a Markov model or similar can be developed, but this is left to future research.

**Table 1. Path Loss Models for MR1 and MR2**

| | | $d_{BP}$ | $\gamma$ | MSE |
|---|---|---|---|---|
| BS1MR1 | NLOS | 144 m | 4.13 | 2.1 |
| BS2MR1 | NLOS | 292 m | 4.15 | 8.1 |
| BS1MR2 | LOS/ NLOS | 52 m | 3.40 | 18.0 |
| BS2MR2 | LOS/ NLOS | 141 m | 3.15 | 15.7 |

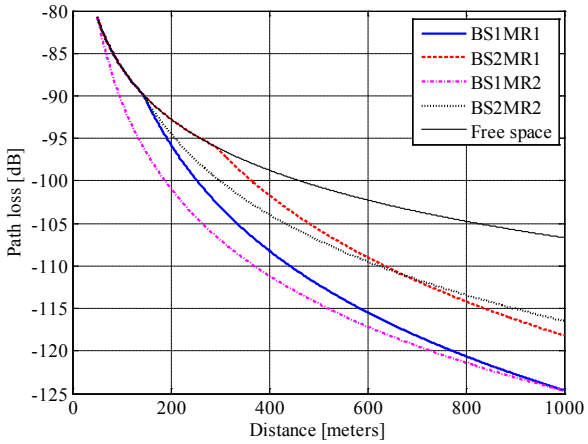


**Figure 7. Comparison between Path Loss Results**

## Statistical Channel Modeling

In this section we will present statistical channel models, that is, models that describe small scale fading characteristics. Shadowing, which also is subject to statistical modeling, is not addressed here. Two different NLOS scenarios will be addressed: One where the BS is placed at a height of 12 meters, and one where the BS height is 38 meters. In most practical situations the mobile station will experience these two environments in quick succession, but a joint modeling is not deemed practical.

### *Theoretical Background*

The distribution of the channel attenuation, and consequently the signal-to-noise ratio, can be shown to typically fall into one of two theoretical distributions. NLOS channels are typically represented as Rayleigh-distributed and LOS channels follow a Rice distribution. In practice other distributions like Weibull and Nakagami-m can show a better fit to the data, but in this work we are mainly

interested in the Rician K-factor as an indication of the presence of a LOS component.

A full statistical model of the LOS/NLOS channels is not viable, nor would it be very useful as the complexity would be hard to manage. Instead a set of parameters relevant to a practical communication system is extracted from the channel measurements. Below is a description of the parameters that will be addressed in this paper:

**Delay spread and transfer functions.** The delay spread function, $h(t,\tau)$, also called the input delay spread [3] and time-varying channel impulse response, gives the channel input/output relationships by

$$y(t) = \int_0^\infty x(t-\tau)h(t,\tau)d\tau.$$

The channel measurements recover a sampled version of this function. From the Delay spread function, we can derive the transfer function, $H(t,\omega)$, which is the Fourier transform of $h(t,\tau)$ over $\tau$. The transfer function is then the instantaneous frequency response of the channel at time $t$.

**Power delay profile (PDP).** The power delay profile $P_t(\tau)$ is derived from the delay spread function as

$$P_t(\tau) = |h(t,\tau)|^2,$$

and gives a measure $P_t(\tau)d\tau$ of the multipath power distribution.

**RMS Delay spread.** The root-mean-square (rms) delay spread is a measure of the amount of multipath components in an environment and their relative strength. The rms delay spread is computed as

$$\tau_{\text{rms}} = \frac{\sqrt{\int_0^\infty (\tau-\bar{\tau})^2 P(\tau)d\tau}}{\int_0^\infty P(\tau)d\tau},$$

where

$$\bar{\tau} = \frac{\int_0^\infty \tau P(\tau)d\tau}{\int_0^\infty P(\tau)d\tau}.$$

Here $P(\tau)$ is the power delay profile of the channel with the time subscript omitted for clarity. Large delay spreads may indicate the need for special precautions in the system design, such as complex channel equalization in the receiver for single carrier systems, or long cyclic prefixes for OFDM systems.

**Doppler spread.** The time-varying fading process has a dual description as a Doppler spectrum. This spectrum will typically have a mean depending on the Doppler shift, given by

$$f_D = \frac{v}{c} \cdot f_C.$$

Here $v$ is the mobile station velocity, $c$ is the speed of light, and $f_C$ is he carrier frequency. The formal definition of the Doppler spread is the rms variation around this mean, and has an impact on e.g. fade durations and pilot schemes. Since the rms Doppler spread will depend on the size of the analysis window, we use an alternative measure, namely the 3 dB bandwidth around the Doppler mean.

**Frequency correlation function (FCF).** The FCF describes the correlation between different frequencies in the transfer function $H(t,\omega)$. That is,

$$FCF(\Delta\omega) = E_t[H(t,\omega)H^*(t,\omega+\Delta\omega)],$$

where the expectation is taken across time. It should be noted however, that this formulation is only valid if the scatterers are uncorrelated, that is,

$$E[h(t,\tau_1)h^*(t,\tau_2)] = 0, \forall \tau_1 \neq \tau_2.$$

In the case of correlated scatterers, we compute the 2-dimensional frequency correlation estimate given below. The main application of the FCF is to find the correlation bandwidth, $B_C$, from which an irreducible error floor in a receiver can be estimated.

**Frequency correlation estimate (FCE)**. The FCE is an alternative to the frequency correlation function (FCF), which is only available when uncorrelated scatterers can be assumed [4]. It is a 2-dimensinal function defined as

$$FCE(\omega_{\text{ref}},\omega_i) = \sqrt{\frac{\gamma(\omega_{\text{ref}},\omega_i)}{\gamma(\omega_{\text{ref}},\omega_{\text{ref}})\gamma(\omega_{\text{i}},\omega_i)}},$$

where

$$\gamma(\omega_i,\omega_j) = \frac{1}{N}\sum_t H(t,\omega_i)H^*(t,\omega_j).$$

When the FCE is computed, it can be used to determine the correlation bandwidth, $B_C$, for any center frequency $\omega_{\text{ref}}$.

### *NLOS Measurements*

In this section we present the channel model parameters obtained from a subset of the BS1 MR1 dataset. The subset consists of measurements at distances between 300-400 meters and is believed to be strictly NLOS at all times.

The data consists of 23 one-second chunks of data, every chunk having 3366-3367 power delay profiles. The GPS position is available at the beginning of each chunk and is used to determine the speed and direction of the mobile station. Assuming approximately constant movement over the one second duration, each PDP is corrected for tilting in the time-delay plane. Allowing too much tilt would cause the taps at different delay to "drift", causing statistics from several taps to be mixed during the analysis.

The first processing step is to extract the real multipath echoes from the noise. Here we use the constant false acceptance rate (CFAR) methodology from [5]. We accept one false echo per 100 PDPs, and also reject all echoes below 25 dB from the strongest component. Examples of the delay spread function before and after this processing is given in Figure 8.

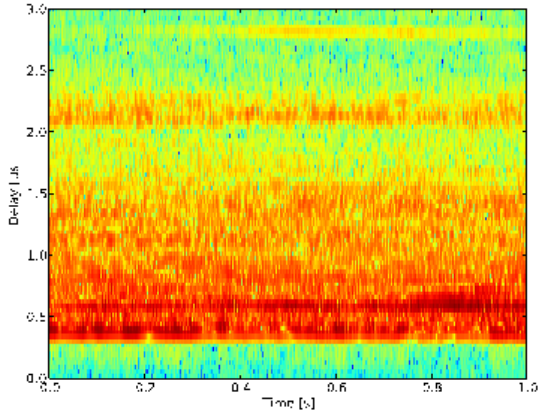

**Figure 8. Delay Spread Function Before Denoising**

Given the filtered delay spread function, we compute the normalized PDPs for the data set. Clearly, as seen by Figure 9, the actual echoes may be very sparse for higher lags and would best be described by a more complex model featuring an underlying Markov chain. However, a simple mean PDP will give a good picture of the power distribution across multipath delays. The mean PDP is computed by normalizing every PDP to have a total power of one. The mean of these normalized PDPs are then computed and is shown in Figure 10, together with its the cumulative distribution.

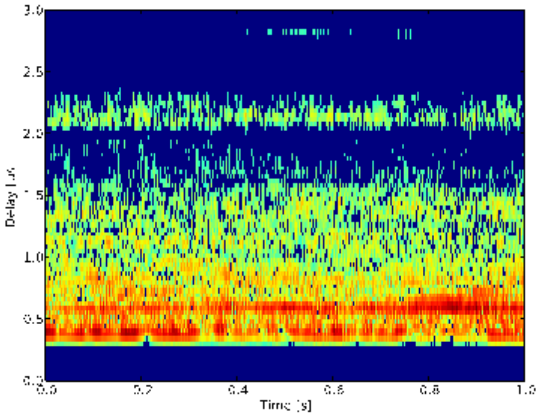

**Figure 9. Delay Spread Function After Denoising**

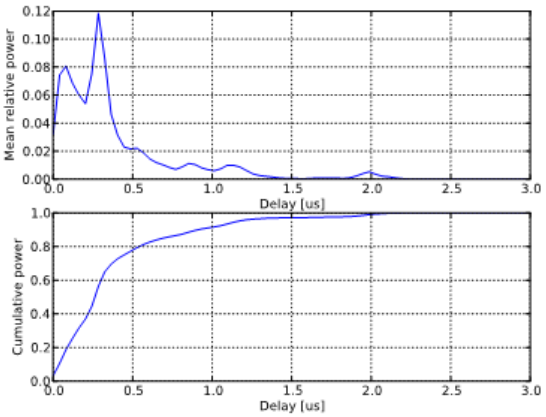


**Figure 10. Mean and Cumulative PDP**

The denoised delay spread function is also used to compute the rms delay spread. A plot of the rms delay spread for the data in Figure 9 is presented in Figure 11 along with its histogram. We can see from the histogram that for this snapshot, most of the rms delay spreads are between 200-400 nanoseconds.

The rms delay spread for the entire dataset is summed up in the histogram in Figure 12. The corresponding minimum, median and maximum delay spreads are 0.06, 0.33 and 0.80 microseconds respectively. A delay of 0.33 microseconds corresponds to 100 meter extra path length.

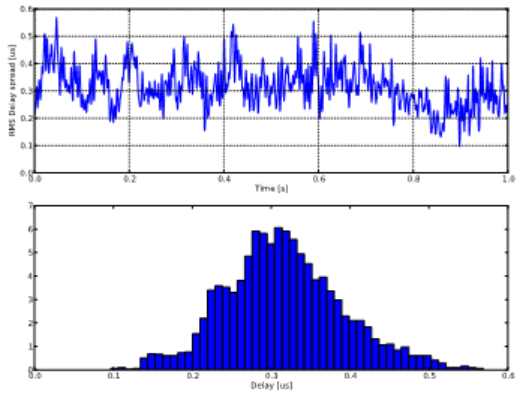


**Figure 11. RMS Delay Spread and Histogram**

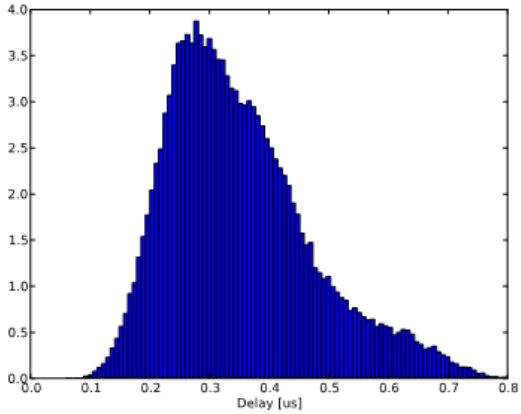


**Figure 12. RMS Delay Spread Histogram**

The Doppler spread is computed using 256 sample blocks, which is equivalent to a time window of 76 milliseconds. The maximum speed of the mobile station is in the order of 10 m/s, making the distance traveled approximately 76 cm. This improves the likelihood that the data being analyzed are follow a stationary process. The signal wavelength on the other hand is 6 cm, so the process should decorrelate nicely over the analysis window. Also, the raw, unfiltered delay spread function is used due to the fact that removing the noise with a non-linear filter introduces artifacts in the spectrum.

Preliminary investigations show that the first ten taps have median Doppler spreads in the range from 13 to 200 Hz. Low ranges like 13 Hz mean that there is very little variation around the Doppler shift, indicating few scatterers whose sum merely modulates the received signal. Doppler spreads of 200 Hz is in the range of the maximum expected with velocities up to 11 m/s.

As in [1] we have found that the scatterers can be correlated, and so we forego the use of the FCF and compute the FCE instead. The FCE is in general a 2-dimensional function, so we present the subset corresponding to the correlation between the mid-band frequency and the rest of the frequency band. The mean FCE is presented in Figure 13. Here we see that the 1/e correlation bandwidth is about 5 MHz, which indicates that there is a fair amount of correlation across the frequencies.

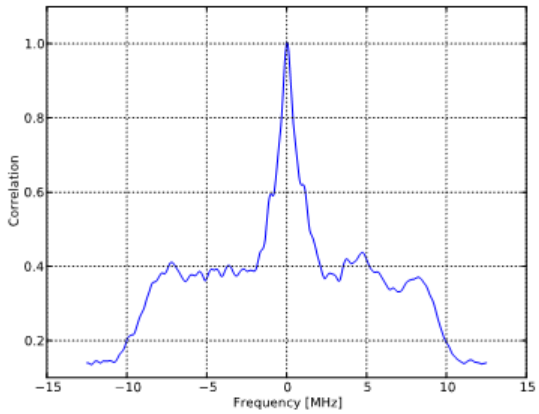


**Figure 13. Frequency Correlation**

The final parameter set that will be presented for the BS1 MR1 dataset are the fading distribution parameters. Although this dataset is assumed to be purely NLOS, which in turn should preclude Rician fading with strong K-factors, the previous results suggest that this may not hold. The K-factors are computed for the 10 first taps, as these hold most of the signal energy.

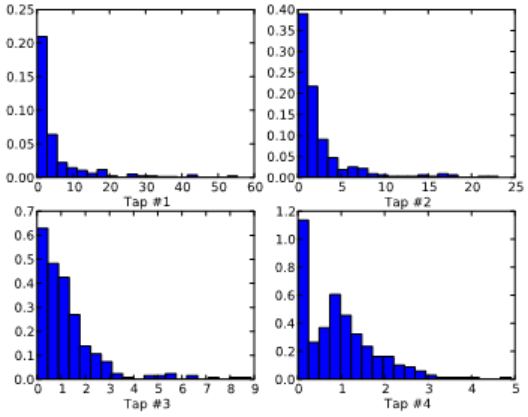


**Figure 14. Histogram of Rice K-Factors**

Figure 14 states that there is indeed a high degree of Rician fading taking place even in this

NLOS case. In [1] term the NLOS-S, or specular NLOS, was introduced in the case where a few strong reflections gave Rician fading even when no direct LOS was available.

Figure 15 tells the same story for the first ten taps. Although the specular component is weak for some taps, there are clearly periods of non-Rayleigh fading for all the taps.

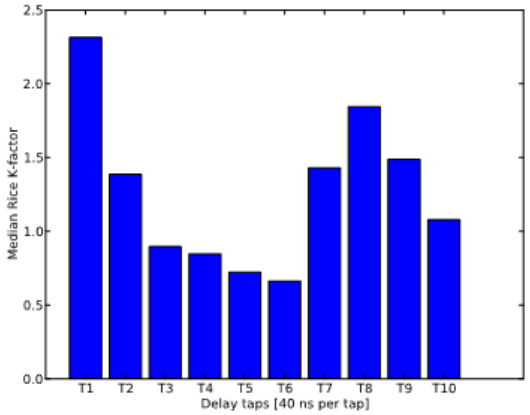


**Figure 15. Median K-Factors for the First Ten Taps**

### *NLOS Measurements for BS2 MR1*

The next set of measurements is taken in the exact same area, but now with the BS antenna at 38 meters.

Visually comparing the non-filtered versus filtered delay spread function for one second of data in Figure 16 and Figure 17, we see that moving the antenna up has shortened the maximum delay of the channel.

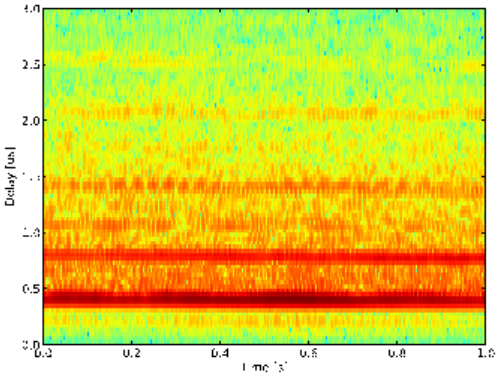


**Figure 16. Delay Spread Function Before Denoising**

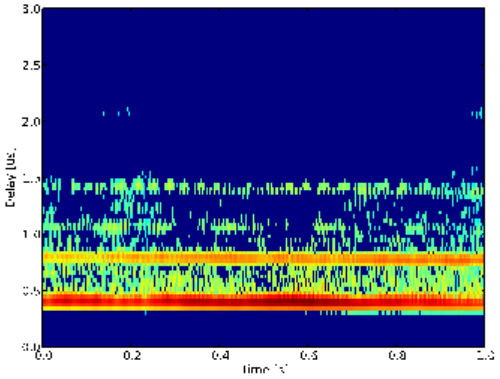


**Figure 17. Delay Spread Function After Denoising**

The same observation can be made when inspecting the mean power delay profile in Figure 18. Here most of the power is concentrated well below 250 ns, while Figure 10 shows most of the power below 500 ns.

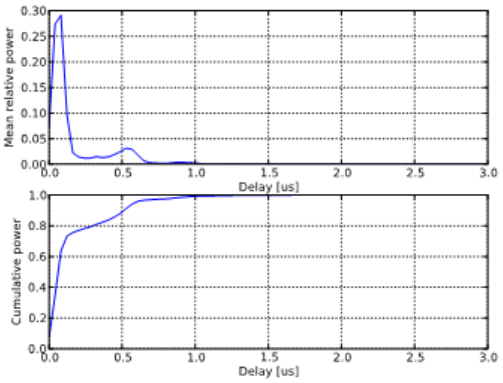


**Figure 18. Mean and Cumulative PDP**

This observation is reinforced when inspecting the delay spread histogram in Figure 19. The minimum, median and maximum rms delay spreads are 31, 179 and 467 nanseconds respectively.

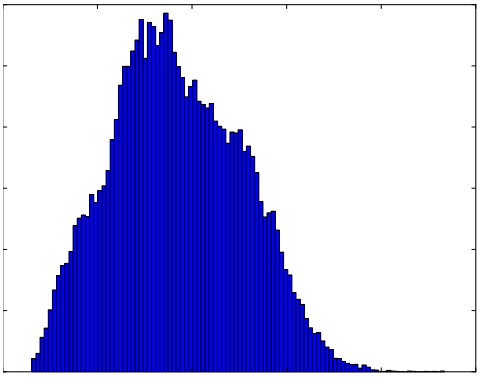

**Figure 19. RMS Delay Spread Histogram**

The Doppler spread follow the same pattern as for BS1 MR1 – lower taps often see pure Doppler shifts, while spreads as high as 190 Hz are seen for higher taps. Again, this suggests that we have little Rayleigh fading for the first few taps.

The FCE for the centre reference frequency is shown in Figure 20. The correlation bandwidth is now close to 20 MHz, which is in line with the reduced rms delay spread.

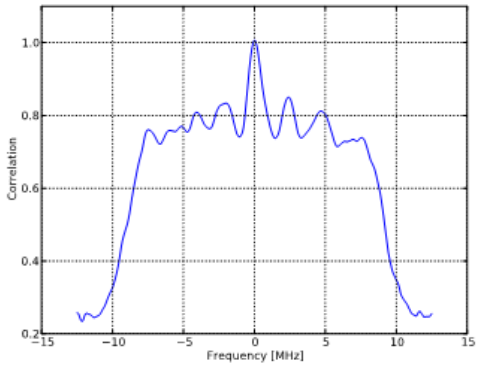


**Figure 20. Frequency Correlation**

The median K-factors shown for the ten first taps in Figure 21 also tell a story of Rician fading. K-factors as high as 80 suggest close to LOS conditions. A reason for this is that the data corresponds to distances between 300 and 400 meters. Comparing with the path loss model for BS2 MR1, we see that 300 meters is just about the break point distance. Hence, this is the area where the channel changes from being basically a LOS channel to a NLOS channel.

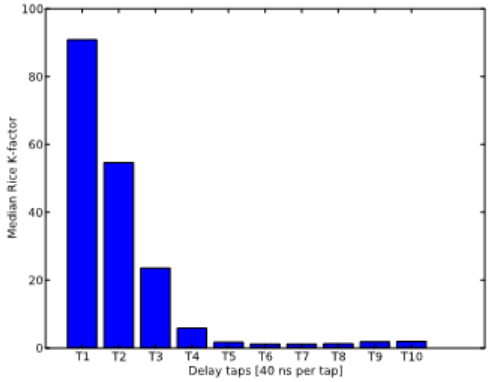


**Figure 21. Median K-Factors for the First Ten Taps**

## Conclusions

In this paper measurement data and corresponding channel characterization have been presented.

The path loss measurements along the terminal building within the gate area show good match with a typical NLOS environment model, represented by a two-slope linear model with path loss exponent about 4.15. The path loss is reduced when the BS antenna height is increased. This effect is well modeled by reducing the break point distance. For communications in a mixed LOS and NLOS environment between parked aircrafts, the data match less with a two-slope linear path loss model. This is as expected, as the path loss is greatly affected by whether there is line-of-sight or not between transmitter and receiver. The average path loss exponent is considerable lower than for the NLOS case. In a continuation of this work, more advanced modeling of the mixed LOS/NLOS path loss will be provided.

For the case of an NLOS channel, the elevated base station gave rise to more Rician fading than the lower position. NLOS conditions seen during these measurements suggest that the scattering environment is less rich than in other cases, with a few strong scatterers often dominating the channel.

## References

[1] D. W. Matolak, Wireless Channel Characterization in the 5 GH Microwave Landing System Extension Band for Airport Surface Areas. 2006.

[2] S. Gligorevic, R. Zierhut, T. Jost, and Wei Wang, "Airport channel measurements at 5.2GHz," Antennas and Propagation, 2009. EuCAP 2009. 3rd European Conference on, p. 877-881, 2009.

[3] P. Bello, "Characterization of Randomly Time-Variant Linear Channels," Communications Systems, IEEE Transactions on, vol. 11, no. 4, p. 360-393, 1963.

[4] R. Bultitude, "Estimating frequency correlation functions from propagation measurements on fading radio channels: a critical review," Selected Areas in Communications, IEEE Journal on, vol. 20, no. 6, p. 1133-1143, 2002.

[5] E. Sousa, V. Jovanovic, and C. Daigneault, "Delay spread measurements for the digital cellular channel in Toronto," Vehicular Technology, IEEE Transactions on, vol. 43, no. 4, p. 837-847, 1994.